Per. Mineral. (2003), *72*, SPECIAL ISSUE: *Eurocarb*, **181-204** http://go.to/permin

PERIODICO di MINERALOGIA
established in 1930

An International Journal of
MINERALOGY, CRYSTALLOGRAPHY, GEOCHEMISTRY, ORE DEPOSITS, PETROLOGY, VOLCANOLOGY
and applied topics on *Environment, Archaeometry* and *Cultural Heritage*

Texture and mineralogy of tuffs and tuffisites at Ruri Volcano in western Kenya: a carbonatite, melilitite, mantle-debris trio

FRANCESCO STOPPA[1]*, GIANLUIGI ROSATELLI[1], FRANCES WALL[2] and MICHAEL J. LE BAS[3]

[1] Dipartimento di Scienze della Terra, Università G'd'Annunzio, via dei Vestini 30, 66013 Chieti, Italy
[2] Department of Mineralogy, The Natural History Museum, Cromwell Road, London, SW7 5BD, UK
[3] School of Ocean and Earth Science, Southampton Oceanography Centre, Southampton University European Way, Southampton, SO14 3ZH, UK

ABSTRACT. — Ruri is located in the Kavirondo rift, near Homa in western Kenya It is a twin volcano with an ijolite-sövite core in its northern half, coupled with a carbonatite-melilitite pyroclastic centre in the southern half. The petrography and mineral chemistry of pyroclastic rocks from the collection of Ruri material at The Natural History Museum, London, have been studied in order to learn more of the nature of the volcanic activity and the erupted magmas

Four types of tuffs have been recognised at South Ruri, on the basis of rock structure and texture, the nature of fragmental materials and matrix relationships: 1- *heterolithic tuff*: a mixture of accidental fragments with no discrete physical juvenile component; 2- *pelletal tuff*: heterolithic tuff with a carbonatitic matrix, with a minor juvenile component of rounded melilititic lapilli cored by mafic HP xenocrysts; 3-*lapilli tuff*: formed mainly of juvenile lapilli, with concentric melilitite layers around a kernel of clinopyroxene or Cr-spinel, immersed in a carbonatite ash-matrix; 4-*lapilli-ash tuff*: mostly microporphyritic carbonatite lapilli in a micritic carbonatite matrix (ie. extrusive carbonatite). Types 1 to 3 are interpreted as conduit and/or vent facies and type 4 is a surge deposit.

The juvenile components of the deposits are of melilititic-carbonatitic type. Their proportion increases with eruptive sequence, indicating a progressively shallower level of magma fragmentation in the conduit. The juvenile silicate material is a feldspar-free association of melilite (now altered) and olivine, with foids, although these are also highly altered. Clinopyroxene, phlogopite and amphibole are slightly fresher. Some Cr-rich clinopyroxene, phlogopite, olivine and chromite have strain features and compositions indicating they are from disaggregated mantle xenoliths

The melilititic melts were co-eruptive with igneous carbonate at Ruri They may represent a small volume, near-primary magma that erupted directly from the mantle, whereas the subvolcanic rocks at Ruri are more differentiated, as are the carbonatites and nephelinites of the nearby Kisingiri stratovolcano. Ruri adds another example to the general pattern that the most primitive magma compositions are erupted at small centres adjacent to the large alkaline/carbonatitic volcanoes. Other examples are Deeti, close to Kerimasi and the Monticchio Lakes at Vulture.

At the liquidus temperature and low pressure of melilitite stability, carbonatite is not a miscible phase and may have erupted as mechanically separated, fine sprays of droplets and ash fragments that now form the matrix of the tuffs, as well as discrete porphyritic carbonatite lapilli.

RIASSUNTO. — Ruri è ubicato nel rift di Kavirondo nelle vicinanze di Homa nella porzione occidentale del Kenia. Si tratta di due piccoli vulcani gemelli, di cui quello settentrionale mostra un complesso subvulcanico di jolite e sövite mentre il secondo conserva rocce piroclastiche di tipo carbonatitico e melilititico. Sono state studiate le rocce conservate al Museo di Storia Naturale di Londra che formano la collezione di Ruri. Lo studio si è concentrato sul significato dell'attività vulcanica verificatasi a Ruri e sulla natura dei prodotti eruttati.

È stato possibile riconoscere quattro tipi diversi di depositi piroclastici nel vulcano meridionale, in base

* Corresponding author, E-mail: fstoppa@unich.it

alle differenze riscontrate tra struttura e tessitura, natura dei piroclasti e relazioni tra clasti e matrici. Essi sono: 1- tufi eterolitici: una mistura di frammenti accidentali priva d'evidenze fisiche di una componete juvenile; 2- tufi pelletoidali: come sopra ma con presenza di una matrice carbonatitica e una frazione silicatica juvenile composta di lapilli sferici nucleati da xenocristalli d'alta pressione; 3- Tufi a lapilli: essenzialmente costituiti da lapilli juvenili di tipo tuffisitico, con gusci concentrici di melilitite intorno ad un nucleo di Cr-diopside o cromo-spinello. I lapilli sono immersi in una matrice carbonatitica; 4- tufi cineritici a lapilli: lapilli carbonatitici porfirici in matrice cineritica carbonatitica (es. carbonatite estrusiva). I tipi da 1 a 3 rappresentano principalmente facies di condotto o crateriche, il quarto è un deposito da ondata piroclastica.

La componente juvenile è sempre costituita da prodotti carbonatitico o melilititico la cui abbondanza cresce progressivamente nella sequenza eruttiva indicando che il livello di frammentazione magmatica diventava via più superficiale nel condotto. Petrograficamente si tratta d'olivin melilitite con foidi; questi minerali sono generalmente alterati. Il clinopirosseno, la flogopite e l'anfibolo sono molto più freschi. Il clinopirosseno ricco in cromo, la flogopite, l'olivina e la cromite mostrano deformazioni intracristalline e hanno una composizione che suggerisce che essi siano derivati dalla disgregazione di xenoliti mantelliche.

Melilitite e carbonatite sono co-eruttive a Ruri rappresentando un esempio di piccolo impulso magmatico primario eruttato direttamente da profondità mantelliche. Invece le rocce sub-vulcaniche mostrano un grado di differenziazione molto maggiore così come le nefeliniti del vicino volcano Kisingiri. Ruri si aggiunge alla lista degli esempi di magmi molto primitivi eruttati da piccoli centri monogenici associati a grandi strato vulcani di natura alcaline ma più evoluta.

Alla temperature del liquido melilititico il carbonato non è miscibile e può essere eruttato separatamente sebbene frammisto a frammenti melilititici. Infatti esso per la sua bassa viscosità tende a formare goccioline e sottile cenere che entra poi a formare la matrice dei tufi melilititici di Ruri.

KEY WORDS: *melilitite, carbonatite, tuffisite, mantle debris, Homa - Kenya.*

INTRODUCTION

Phonolite-nephelinite-carbonatite, and their respective intrusive terms ijolite-sövite associations in western Kenya have been studied in detail by Le Bas (1977). However, these rock suites are usually considered to represent differentiated magmas and are thus unlikely to be near-primary parental magma compositions. This is consistent with a lack of mantle xenoliths.

The possible significance of the melilitite/carbonatite association, which is present in the western branch of the East African rift, has received scant attention in the eastern branch of the rift. However, melilititic assemblages have been recognised in satellite monogenetic volcanoes scattered around large nephelinite/phonolite stratovolcanoes in western Kenya (Le Bas, 1977; Clarke and Roberts, 1986). At Lake Simbi maar crater (Homa Mountain area), wehrlite xenoliths coated with melilitite represent likely mantle material. At the Got Chiewo vent on Homa Mountain, melilitite flows and agglutinated carbonatitic tuff are interstratified (Keller, 1989). Similar extrusive carbonatite occurs on the southern rim of the South Ruri crater. Since the comprehensive description of western Kenyan volcanism by Le Bas (1977), much more work has been done on extrusive carbonatites worldwide. Most have been found to be calcite carbonatites although they tend to have higher silicate contents and less extreme compositions than many intrusive carbonatites. Unfortunately they are prone to alteration and can be difficult to study. The natrocarbonatite lavas of Oldoinyo Lengai are the best-known example of extrusive carbonatites but are unique in being highly alkaline. Whilst most intrusive carbonatites may be the cumulate products of fractionated melts, most of the extrusive carbonatites are the quenched products of high temperature liquids. An increasing number of extrusive carbonatites have been found to be closely associated with silicate rocks, mainly melilitite and, in some cases, phonolite (Woolley, 2002).

The Ruri complex is a good example of a co-eruptive association of alkali mafic silicate rocks and carbonatites within a small area (Le Bas, 1977). A large collection of Ruri rocks (1200) is

housed in the Natural History Museum, London; about two thirds of these are intrusive and country rocks: the former comprise mainly coarse-grained carbonatite (sövite), fine-grained calcite carbonatites (alvikite), ferro- and similar late stage- carbonatites, plus phonolite, nepheline syenite, ijolite, melanephelinite. The remainder are pyroclastic rocks; their nature and mineralogical composition form the subject of this contribution.

GEOLOGICAL BACKGROUND

The Ruri outcrops are situated near the Kenya-Uganda border, near the northeast shoreline of Lake Victoria. Ruri is one of the three main alkaline-carbonatitic complexes of the Homa Bay District, the others being the Homa Mountain centre and the large stratovolcano of Kisingiri, with its central Rangwa caldera (Le Bas, 1977). The Homa district lies within the Kavirondo Rift, which is a westward branch of the Gregory Rift, extending for about 160 km towards Lake Victoria (Fig. 1).

Part of the North and South Ruri vents consists of proximal inward-dipping crater tuffs and conduit breccias (Fig. 2). Outward-dipping crater facies are preserved only on the southeast side of South Ruri. A few small outcrops of water-lain «epiclastites» provide

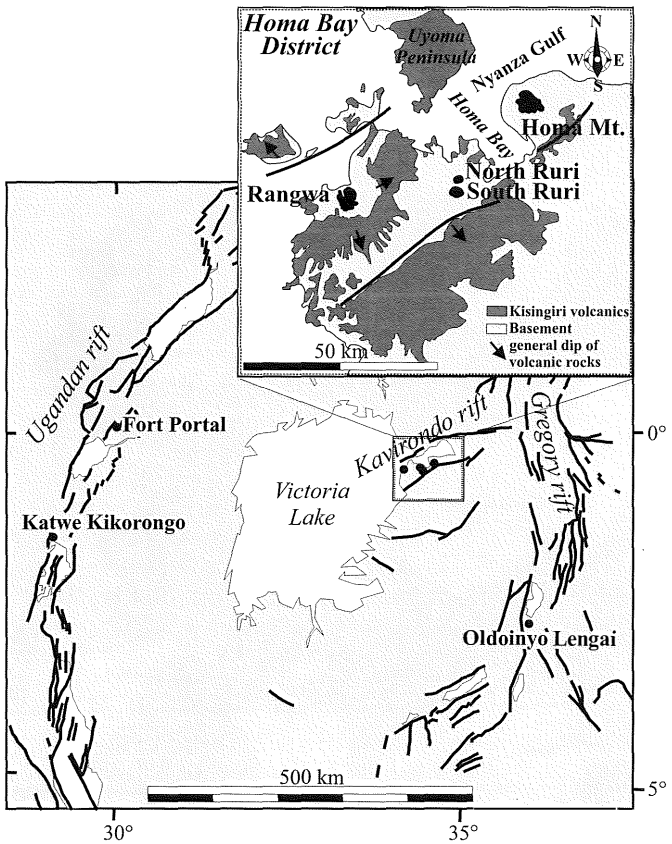

Fig. 1 – Sketch-map of the East African Rift with the location of Ruri and the other volcanoes of the Homa Bay volcanic district.

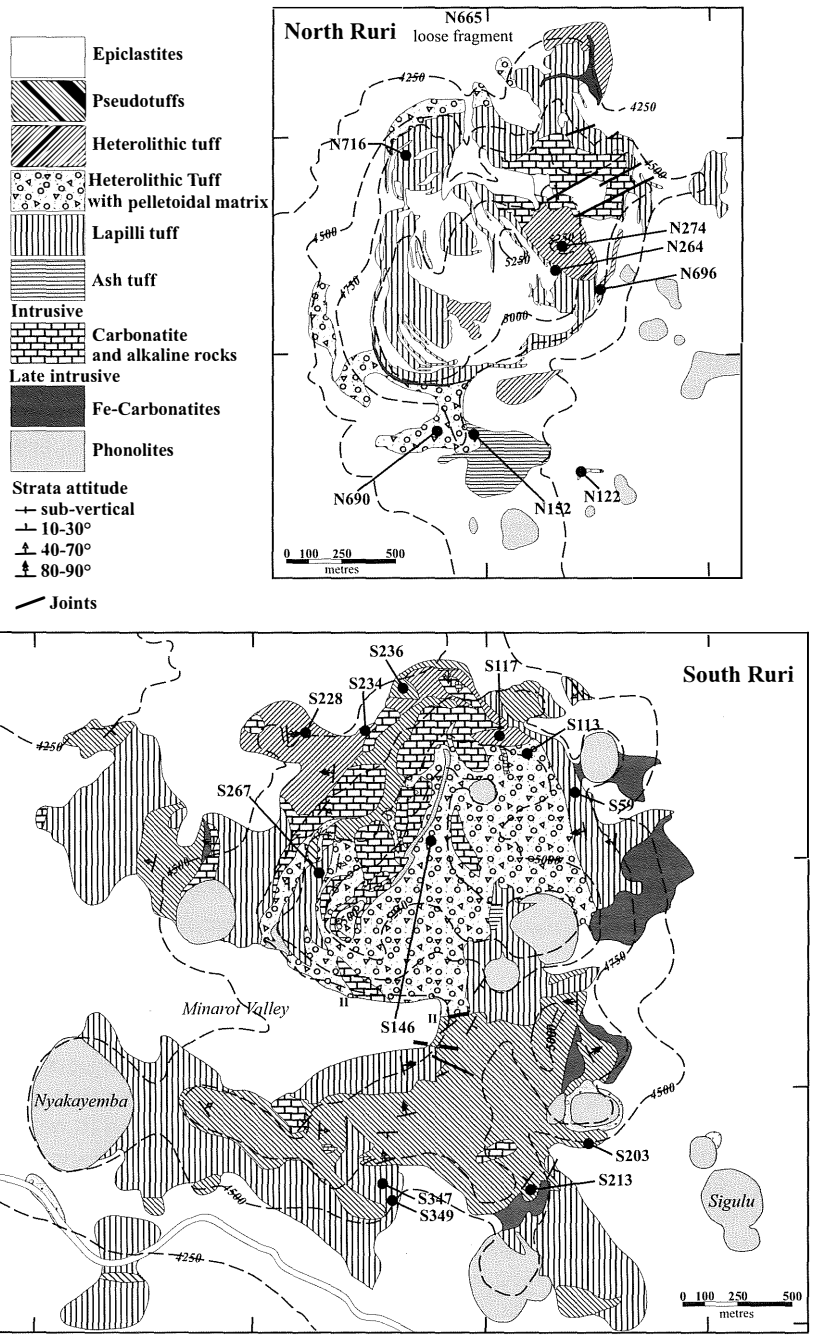

Fig. 2 – Geological maps of the North and South Ruri volcanic complexes. Redrawn from the original fieldwork of Dixon and Collins. In the maps are reported only the samples that could be placed unambiguously at the original sampling site.

evidence of the former presence of a crater lake at South Ruri, but later plugs of carbonatite obscure much of the vent area. There are no traceable lava flows (Le Bas, 1977). There is no reason to make a genetic distinction between North Ruri and South Ruri. They may represent two small twin volcanoes, or even separate conduits or vent areas of the same monogenetic volcano. Numerous late-stage phonolite plugs occur in the vicinity of the Ruri Hills, they have no clear relationship to the explosive activity, although some of them were emplaced in Ruri conduits. Mutual crosscutting relationships indicate that some of the subvolcanic carbonatites and the phonolite are closely related, both spatially and temporally

METHODOLOGY

The Ruri collection is identified here by the original field numbers corresponding to references in Le Bas (1977). Each sample is located on a topographic base map (Fig. 2), following the original fieldwork by Dixon and Collins. Four hundred extrusive rocks were examined in hand specimen and in thin section, 23 were considered representative and are described here in terms of structure and texture, with 13 finally chosen for detailed electron microprobe study. The electron microprobe analyses were performed using a Cameca SX50 wavelength-dispersive electron microprobe at The Natural History Museum, using a variety of synthetic materials and natural minerals as standards and a $\phi\rho\zeta$ matrix correction programme. About 200 analyses were made and a selection of about 50 is presented here. Laser Ablation Inductively Coupled Mass Spectrometry (LA ICP MS) on amphibole S113, was carried out at Kingston University. The CETAX LSX 100 Nd:YAG laser, built by Surrey Design Research Instruments, operated at 266 nm wavelength, with a working energy of 0 15-0 2 mJ/pulse The data acquisition was carried out in peak jumping mode (Rosatelli, 2002). For the data processing CaO, independently determined by EMPA, was used as an internal standard NIST SRM 610 and NIST SRM 612 were used as external standards. In the data correction procedure, both inter-element fractionation and the difference of mass ablated in each analysis were considered following the procedure of Longerich *et al.* (1996).

LITHOLOGY

The nomenclature of pyroclastic rocks is based on current clast size criteria (IUGS, Le Maitre, 2002). However, considering the ultramafic nature of the rocks, their mixed composition and occurrence, specific attention has been paid to matrix-clast relationships, lapilli shape and the internal structure of lapilli. Specific nomenclature, textural classification, and genetic classification criteria have been adopted following the suggestions of Mitchell (1997).

PSEUDOTUFFS
(AUTOBRECCIATED RHEOMORPHIC ALVIKITE)

Ref sections S236, S203, S181 (not on map)

A tuff formed by subangular- to plastically-shaped polycrystalline carbonate clasts The clasts contain relict structures of unknown origin, consisting of well-defined, rounded areas of very fine opaque granulation which are typical of Ruri alvikites and may correspond to discrete carbonatite «pseudolapilli». The clasts are arranged in a faintly eutaxitic texture. A very minor proportion of halloclasts (accidental lithics), probably host rocks, are present in one sample (S203) but all the others are monolithic. A similar facies from Homa has already been interpreted as a spatter lapilli facies (Keller, 1989). However, the «pseudolapilli» do not have internal signs of flattening or of fluidal arrangement The rock matrix forms a continuous groundmass, it is not obviously granular and shows no volcanic gradation.

Taking into consideration the field evidence, a rheomorphic brecciation of alvikite dykes seems the most likely origin of these rocks.

HETEROLITHIC TUFFS (MAPPED, OR PREVIOUSLY CLASSIFIED, AS EXTRUSIVE CARBONATITE TUFFS)

Ref sections N274, N696, S234/1, S370 (not on Fig 2), S228/2, S117

These are breccias having angular or subangular, mainly lapilli-sized, clasts. The following lithic clasts are present in very variable amounts: metabasalts with various degrees of alteration and granularity; smaller holocrystalline doleritic fragments; nepheline syenite; orthoclasite; fenite. The matrix consists of cleavage fragments of clinopyroxene, K-feldspar, apatite, and kink-banded phlogopite. Mafic minerals are partially replaced by calcite. Fine-grained alvikite fragments form a large part of the matrix. Cryptocrystalline, turbid carbonate rich in Fe-oxides and apatite forms the intergranular component. In some places, the matrix has recrystallised into sparry carbonate. There are no obvious juvenile lapilli but the carbonatite matrix and mineral fragments may include a juvenile physical component. The rock may be interpreted as a conduit or vent deposit.

HETEROLITHIC TUFFS WITH PELLETAL MATRIX (TUFFISITE)

Ref sections N690 N122 N380 (not on Fig 2, S146, S113)

Heterolithic tuffs contain subangular, accidental lithic clasts similar to those of the group above. Large altered olivine crystals, clinopyroxene and fresh amphibole, up to 2 cm diameter, also occur as mega-xenocrysts. These rocks have a distinct matrix structure and an apparent juvenile component that consists of welded or agglutinated glassy or carbonated micro-lapilli with a kernel at their centre. Apatite is the only fresh mineral in the groundmass of the lapilli. The lapilli are rounded or oval and sometimes have a thin altered glassy veneer, giving the rocks the appearance of a pelletal tuff. The matrix comprises ash-sized glassy droplets and rounded mafic minerals (Fig. 3A). The latter are mainly spinel, clinopyroxene and phlogopite. The mafic minerals exhibit undulose extinction and corona reactions, and the phlogopite flakes are deformed. The matrix is composed of turbid microcrystalline carbonate that encloses the pelletal lapilli. Some intergranular spaces are filled with monocrystalline calcite cement.

From these characteristics, especially the heterolithic nature and the pelletal texture, this rock may be interpreted as a tuffisite. This implies that it is a vent or conduit infilling. A CO_2-fluidised convoy of country rocks and melt droplets plus ultramafic debris is considered likely to have produce this sub-volcanic tuff (Stoppa *et al.*, this volume). Such rocks are a common feature of kimberlites, melilitites and carbonatites infilling diatremes (Mitchell, 1997).

LAPILLI TUFFS

Ref Sections S59/3, S267, S347, S349, N716, N264, N660

These rocks contain minor amounts of subangular metabasalt, fenite, orthoclasite, quartzite, and granite fragments. However, a juvenile fraction is dominant and composed of microporphyritic lapilli with an internal concentric fluidal arrangement of former melilite laths. The melilite is altered into a mixture of clay minerals and calcite but shows relict median crack and peg structure. Despite an extensive search no fresh melilite was found. The melilititic lapilli are always rounded and cored by carbonated clinopyroxene or spinel (Fig. 3B and C). It seems that they formed by accretion of melilitite melt shells around a nucleus, rather than from lapilli or drops of magma. Clinopyroxene and phlogopite also occur in the groundmass of the

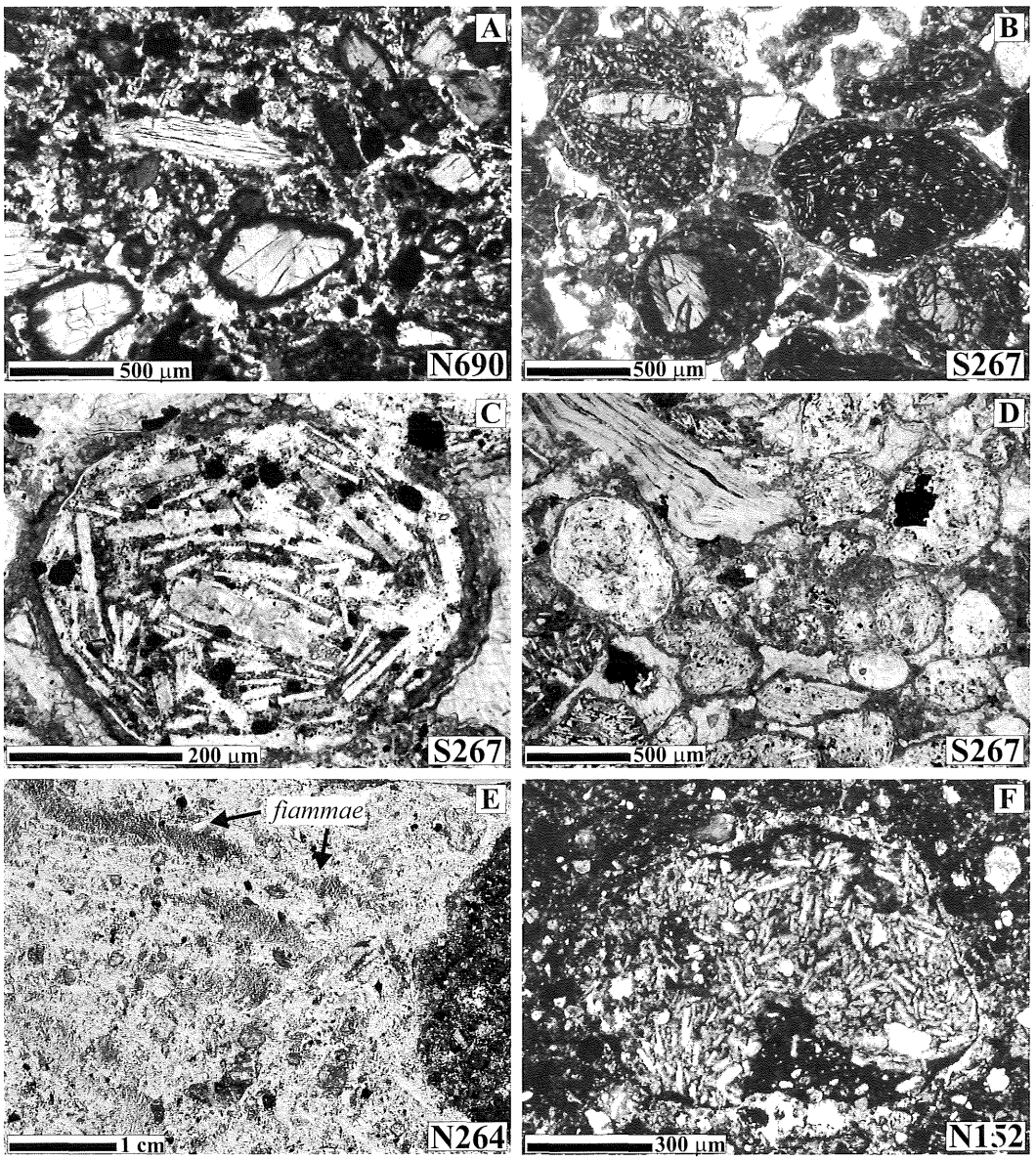

Fig. 3 – Photo table. A) Sample of heterolithic tuff with sub-angular accidental crystals of clinopyroxene and phlogopite in a matrix of micro-lapilli of silicate and carbonate composition plus crystal fragments. B) Lapilli tuff, the lapilli are microporphyritic, often with a kernel of clinopyroxene. C) Microporphyritic lapillus with concentral fluidal arrangment of altered melilitite laths. The larger central crystal although calcitized, has preserved median line and peg structure typical of melilite. D) Agglutinated lapilli with fluidal microporphyritic texture. The upper right lapillus has a Cr-spinel core (sp). In the upper left of the photo there is a deformed phlogopite crystal (phl). E) carbonatite composed of fine grained turbid carbonate matrix in which lumps of carbonate material appear stretched and flattened: fiammae structures. F) Crystal-rich tuff with altered melilitite lapillus. The dark matrix is composed of granular silicate-carbonate material.

lapilli and show a variable amount of carbonate replacement. Lapilli are commonly welded and agglutinated indicating high temperature emplacement (Fig. 3D). In all other cases the lapilli are matrix-supported. The matrix of the tuff consists of fine-grained carbonate and larger calcite single crystals together with euhedral apatite, abundant fine-grained magnetite crystals, clinopyroxene and some perovskite and nepheline fragments. Other completely altered crystals are morphologically similar to olivine. There is a crystal lineation that gives the matrix some fluidal banding, which is a clear sign of plasticity at high temperature. Lapilli of carbonate material are deformed, stretched and flattened to form apparent carbonatite fiamme (Fig. 3E). The latter are immersed in a turbid carbonate matrix. Recrystallised limpid carbonate patches also occur in variable amounts and may represent original vesiculation. The massive texture of this tuff suggests that it may be a high temperature pyroclastic flow.

ASH TUFF

Ref Sections N665 and N152

These tuffs have sand-sized grains and cross-laminated layers. Some layers are crystal-rich ash tuffs with rare acnelithic lapilli. These acnelithic lapilli are mostly composed of carbonatite droplets, suspended in a granular silicate-carbonate matrix. They are considered to be discrete carbonatite lapilli whose rounded or drop shape is dictated by surface tension. Some carbonatitic lapilli have a concentric texture with a fine granular carbonatite core but no crystal kernel, and an external porphyritic rim with carbonate laths in an opaque-carbonate matrix. Other carbonatite lapilli also have a fluidal microporphyritic texture, with densely packed calcite laths that have exsolved fine granular opaque material at their rims (Fig. 3F). They are considered to represent former primary calcite phenocrysts. Some of the small unaltered mica flakes are arranged in a fluidal texture. The matrix material is grain-supported, well-sorted and has minor fine-grained components. Polycrystalline, subrounded calcite or single crystals of calcite could represent fragments of alvikite. The silicate minerals present are sharp, angular fragments of quartz, K-feldspar, clinopyroxene, aegirine and phlogopite. Apatite is also present, as are magnetite and fluorite grains that may have come from original alvikite or ferrocarbonatite clasts. These ash tuffs may have been produced by a pyroclastic surge.

MINERALOGY

The hybrid and variable nature of the Ruri tuffisites and tuffs, coupled with the large amount of fenitised fragments and alteration processes, preclude the use of whole rock analyses. However, the mineral composition has been investigated in order to assess the juvenile or accidental nature of the crystals and their relationships with the melt. In order to analyse the different textural occurrences, the following samples were selected: S113, S236, S267, S347, N122, N152, N380, N264, N696, and N716. Mineral compositions from similar African Rift occurrences have been used for comparison, with particular emphasis on compositions from mantle xenoliths.

Olivine

Olivine occurs as altered crystal fragments in the cores of lapilli in pelletal tuff and lapilli tuff. Prismatic or rounded pseudomorphs after olivine are common and consist of Fe-oxide plus calcite. However, a few fresh forsteritic cores have been analysed in sample S267 (Table 1). Their CaO content is low, around 0.2 wt.%, as are the Cr and Ni contents; but chromite inclusions were found (Tables 1 and 5). The occurrence of olivine in the lapilli cores, corrosion of the margins and replacement by calcite indicate disequilibrium

TABLE 1

Representative analyses of olivine.

sample		**S267**	
analysis	#1	#2	#17
SiO_2	38.98	39.33	39.96
FeO*	15.17	15.05	15.29
MgO	44.58	44.82	43.91
MnO	0.29	0.25	0.24
CaO	0.24	0.19	0.25
Total	99.26	99.64	99.65
Cation calculation based on 4 O			
Si	0.989	0.992	1.007
Fe	0.322	0.318	0.322
Mg	1.686	1.686	1.650
Mn	0.006	0.005	0.005
Ca	0.007	0.005	0.007
Sum	3.010	3.006	2.991
Mg#	0.84	0.84	0.84

FeO* = total iron. Analyses #1 and #2 contain 0.07 and 0.15 wt.% NiO respectively.

with the melt and a possible xenocrystic origin. Olivine xenocrysts of similar composition are known from carbonatitic lavas at Fort Portal (Barker and Nixon, 1989), from olivine-biotite-pyroxenite (OBP) xenoliths at Oldoinyo Lengai and Loluni (Dawson and Smith, 1992), and in garnet and spinel peridotites from Lashaine (Dawson *et al.*, 1970). All of these olivine occurrences have been compared with Ruri using a Mg# vs CaO plot (Fig. 4). Olivine xenocrysts from Fort Portal carbonatite lavas seem to have an inverse correlation between Mg# and CaO which may be the result of reaction with host liquids. Fresh Ruri olivine cores plot near the OBP field, very close to olivine in xenoliths from Oldoinyo Lengai and the most primitive Fo-rich, CaO-poor olivine in Fort Portal carbonatite. Ruri olivines are also similar to the higher Fe and Ca olivines in mantle xenoliths from Lashaine. Therefore, a mantle xenocrystic origin is probable for the Ruri olivine cores.

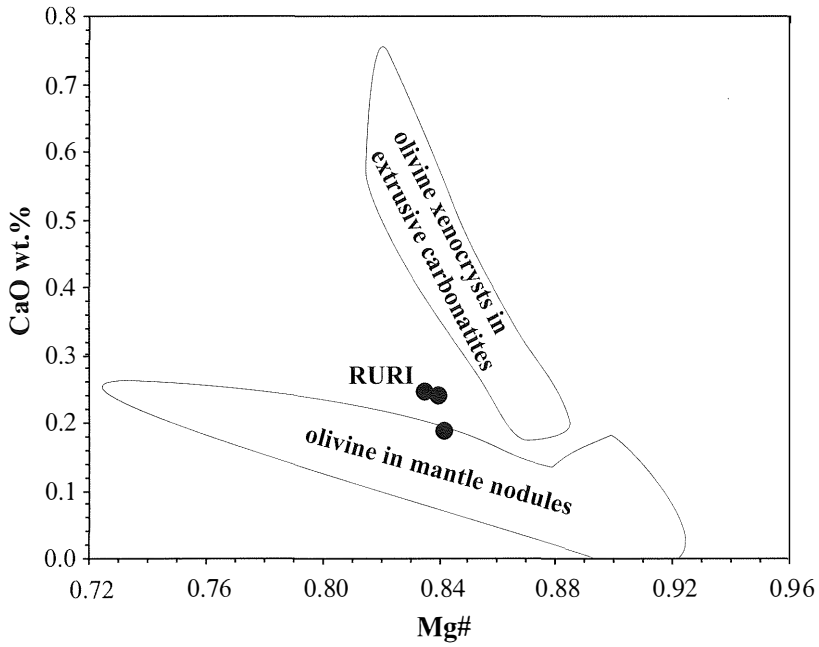

Fig. 4 – Composition of Ruri olivine (S267) with olivine from African extrusive carbonatites and mantle xenoliths. See text for references. The olivine in the Ruri lapilli tuff has Mg# (= $Mg/Mg+Fe^{2+}$) and CaO contents more similar to mantle nodule olivines than olivine xenocrysts in extrusive carbonatites.

Pyroxene

Three distinct groups of clinopyroxene, diopside, salite and aegirine, have been recognised on the basis of texture and composition (Table 2, Fig. 5)

Diopside

Clinopyroxene in pelletal tuff is colourless or pale green Small crystals are generally rounded, strongly corroded and can have a carbonate coating. Larger subhedral or anhedral crystals up to 2 cm in length exhibit a variable degree of fracturing, fine-grained re-crystallization at their rims and undulose extinction (e.g. sample N380). Most of them are coated with altered glass. Twinning is absent and deformed exsolution lamellae are rare, but patchy polarising colours suggest that the crystal lattice is deformed. Trains of tubular fluid inclusions cross-cut the xenocrysts and indicate migration of fluids toward fractures and calcite blebs. This feature has been considered to be an indication of decrepitation and incipient decompression melting during ascent to the surface (Pasteris, 1987) of mantle debris. The xenocrystic diopside in sample N380 (Table 2, anals 1 and 2) has a high Si# and not quite enough Al to fill the T site. It is characterised by a Ca# (=Ca/Ca+Mg) of about 0.5, and a high Mg# ($Mg/Mg+Fe^{2+}$) which is always >90. The diopside is also Cr-bearing, with up to 0.41 wt.% Cr_2O_3. These characteristics, along with the low TiO_2 content (of about 0.6 wt.%) are typical of high pressure xenocrysts in kimberlites and lamproites (Nixon, 1987). Furthermore, the Ruri diopside xenocryst compositions are similar to the compositions of diopside in Northern Tanzania OBP and mantle xenoliths from Deeti (Fig. 6).

Salite

Occasional large clinopyroxene crystals occur at the cores of some melilititic lapilli. Much of the clinopyroxene has been pseudomorphed by calcite but the fresh clinopyroxene is salite (Fig. 5). Salitic clinopyroxenes have also been found as euhedral microphenocrysts in the melilititic pelletal lapilli, and in the tuffisite matrix. The salite crystals are pale brown with a weak green-brown pleochroism, twinned and often have a strong concentric zoning.

In general Ruri salite has lower silica than diopside but higher Al (Table 2, anals. 3-5) T site progressive saturation is coupled to an increase in Ti (TiO_2 = 1-2 wt.%) and Ca# (0.60-0.62) and lower Mg# (0.78-0.84). Quenched salite microphenocrysts in the groundmass of lapilli have higher Ca# (0 60- 0 64), corresponding to a higher Wo molecular proportion (Table 2, anal. 5). They are also poorer in Si, but richer in Ti and Al, than salite cores. The TiO_2 content is around 3.5 wt.%, and Al_2O_3 between 5.9 and 6.8 wt. %. This trend is typically found in leucitites, nephelinites and carbonatite-related melilititic lavas (Cundari and Ferguson, 1982, Stoppa and Principe, 1998) and is considered to be a product of low-pressure, high-temperature crystallization. The systematic enrichment in Al in Ca-rich pyroxenes is generally coupled with depletion in the Si concentration in the host magma (e.g. Kushiro, 1960; Le Bas, 1962).

Aegirine

Green aegirine and aegirine-augite clinopyroxene forms cleavage fragments scattered in the matrix and occur in a variety of fenitised rocks. They are mainly close to the aegirine end-member although one composition plots in the aegirine-augite field (Table 2, anals 6-8 and Fig. 5) They may well all be fenite-derived material.

Phlogopite

Mica phenocrysts occur in many Ruri samples. They are usually brown or dark brown, pleochroic, and have strain features such as kink-banding. Some crystals have resorbed or ragged margins against the matrix. In sample N264 mica is partially replaced by fluorite, aegirine and carbonate. It is considered to be a xenocryst because is does not appear to

TABLE 2

Representative analyses of clinopyroxene.

sample	N380	N380	S113	S113	S267	S236	N152	N152
mineral	Cr-Diop	Cr-Diop	Salite	Salite	Salite	Aeg	Aeg	Aeg
	1	2	3	4	5	6	7	8
SiO_2	53.76	53.88	48.95	44.85	47.85	52.99	52.94	52.81
TiO_2	0.62	0.61	1.48	3.43	0.99	4.00	0.37	0.57
Al_2O_3	1.19	1.16	3.69	6.77	5.52	1.77	0.79	0.19
FeO*	3.30	3.44	9.92	11.45	12.74	-	-	
Fe_2O_3*	nd	nd	nd	nd	nd	27.05	27.36	24.79
Cr_2O_3	0.41	0.26	-	-	-	-	-	-
MnO	0.11	-	0.20	0.28	0.32	0.06	0.36	0.51
NiO	-	0.08	-	-	-	-	-	-
MgO	16.73	16.62	11.06	9.04	8.72	1.08	2.56	4.07
CaO	24.68	24.86	22.97	22.06	19.89	0.81	4.50	8.09
Na_2O	0.49	0.42	1.08	1.41	1.85	13.42	11.58	9.36
Total	101.29	101.33	99.35	99.29	97.88	101.18	100.46	100.39
Si	1.934	1.940	1.846	1.704	1.840	1.981	1.990	2.002
Al	0.050	0.049	0.164	0.303	0.250	0.078	0.035	0.009
Ti	0.017	0.016	0.042	0.098	0.029	0.113	0.010	0.016
Fe^{3+}	0.070	0.061	0.140	0.205	0.152	0.705	0.773	0.641
Fe^{2+}	0.029	0.043	0.173	0.159	0.258	0.055	0.000	0.066
Cr	0.012	0.007	-	-	-	-	-	-
Mg	0.897	0.892	0.622	0.512	0.500	0.060	0.144	0.230
Mn	0.003	-	0.006	0.009	0.010	0.002	0.012	0.016
Ca	0.951	0.959	0.928	0.898	0.819	0.032	0.181	0.329
Na	0.034	0.029	0.079	0.104	0.138	0.973	0.844	0.688
Sum	3.997	3.996	4.000	3.992	3.996	3.999	3.989	3.997
Ca#	0.51	0.52	0.60	0.64	0.62	0.35	0.56	0.59
Mg#	0.97	0.95	0.78	0.76	0.66			
Q	1.88	1.89	1.72	1.57	1.58	0.15	0.33	0.63
J	0.07	0.06	0.16	0.21	0.28	1.95	1.69	1.38
WO	48.76	49.05	49.66	50.38	47.10	3.78	16.33	25.66
EN	45.99	45.61	33.26	28.71	28.74	7.07	12.95	17.95
FS	5.26	5.35	17.08	20.91	24.16	89.15	70.73	56.40
WEF	96.50	97.01	91.62	88.39	85.21	7.16	16.61	31.78
JD	0.00	0.00	0.54	0.38	5.49	7.18	2.65	0.90
AE	3.50	2.99	7.85	11.23	9.30	85.66	80.74	67.33

Diop = Diopside, Aeg = Aegirine. FeO* and Fe_2O_3* = total iron. Fe^{2+}/Fe^{3+} calculated on the basis of charge balance. - = below detection limit estimated as 0.05 wt.%. nd = not determined.

be stable in the host melilititic or carbonatitic pyroclastics.

The Al_2O_3 content of the Ruri micas is generally low, <13 wt.%, and is just enough to fill the tetrahedral site (Table 3). Consequently the mica structure is tri-octahedral and its nomenclature is based on Mg / Fe ratio (McCormick and Le Bas, 1996). TiO_2 is

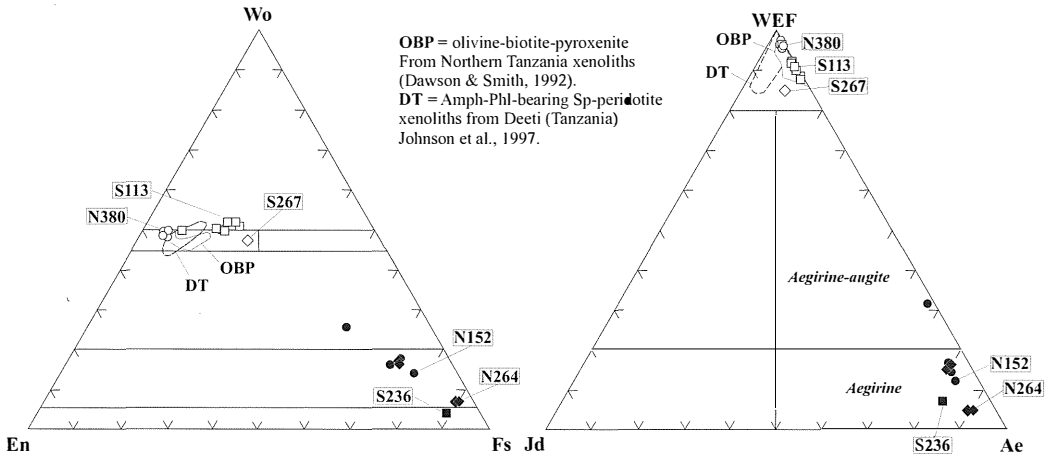

Fig. 5 – Clinopyroxene classification diagram. Enstatite (En)-Ferrosilite (Fs)-Wollastonite (Wo) and WEF-Jadeite (Jd)-Aegirine (Ae) endmembers.

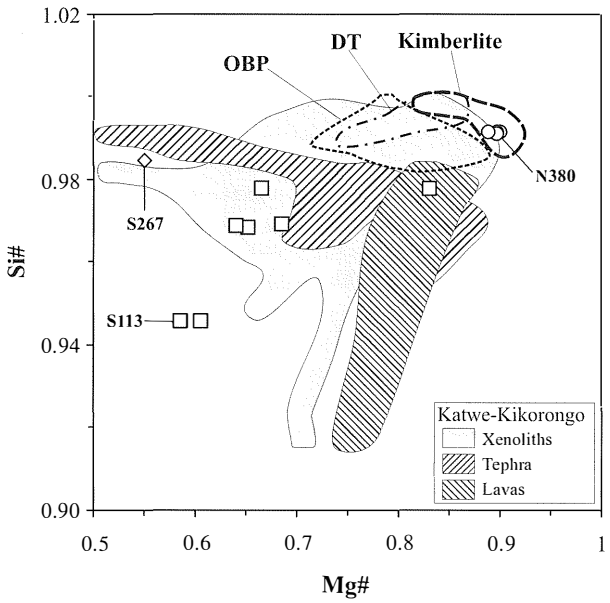

Fig. 6 – Ruri clinopyroxene compositions compared with clinopyroxenes in xenoliths, lavas and tephra of Katwe-Kikorongo, in OBP, in Deeti xenoliths (DT) and in kimberlites. See text for references. Ruri analyses are indicated by sample number.

generally low, below 2 wt.% and only biotite in sample S113 has high TiO_2, up to 4.55 wt. %. An Al_2O_3 vs TiO_2 variation diagram (Fig. 7) is used to compare micas from extrusive carbonatites (Rangwa, Rosatelli *et al.*, submitted; Uyaynah, Woolley *et al.*, 1991), melilitites of the Ugandan rift (Lloyd *et al.*, 2001), fenites at Loe Shilman, India (Mian and

TABLE 3

Representative analyses of mica

sample	N264	N264	N264	N696	N696	S113	S113	S347	S347
analysis	#6	#8	#9	#38	#39	#12	#13	#32	#37
mineral	phl	phl	phl	bio	bio	bio	bio	bio	phl
SiO_2	40.92	42.99	40.85	38.39	37.90	34.84	34.70	44.58	44.67
TiO_2	1.56	1.43	1.64	1.40	1.02	4.46	4.55	0.92	0.70
Al_2O_3	11.23	10.42	10.94	8.29	10.36	12.43	12.68	12.13	10.12
FeO*	5.82	6.72	7.92	21.23	24.07	21.51	21.82	15.46	13.09
MnO	1.72	1.38	2.01	0.55	0.28	0.42	0.46	0.26	0.21
MgO	19.19	19.37	18.20	12.48	9.95	10.45	10.08	12.42	16.79
CaO	0.36	0.13	0.21	0.44	0.29	-	-	0.68	0.44
BaO	1.69	1.21	2.69	0.07	-	0.53	0.52	0.10	0.07
Na_2O	0.27	0.62	1.13	0.28	0.09	0.64	0.58	0.52	0.94
K_2O	9.82	9.58	8.76	9.68	10.00	9.28	9.16	8.14	8.65
F	3.87	3.85	3.46	1.93	1.59	0.49	0.58	1.94	2.81
Total	96.45	97.70	97.81	94.74	95.55	95.05	95.13	97.15	98.49
				Cation calculation based on 22 O					
Si	6.143	6.324	6.116	6.151	6.058	5.513	5.494	6.533	6.492
$Al^{[IV]}$	1.857	1.676	1.884	1.564	1.942	2.316	2.364	1.467	1.508
$Al^{[VI]}$	0.128	0.129	0.045	0.000	0.008	0.000	0.000	0.626	0.224
Ti	0.176	0.158	0.185	0.169	0.123	0.531	0.542	0.101	0.077
Fe^{2+}	0.731	0.827	0.992	2.845	3.218	2.846	2.889	1.895	1.591
Mn	0.219	0.172	0.255	0.075	0.038	0.056	0.062	0.032	0.026
Mg	4.295	4.248	4.062	2.981	2.371	2.465	2.379	2.713	3.638
Ca	0.058	0.020	0.034	0.076	0.050	-	-	0.107	0.069
Ba	0.099	0.070	0.158	0.004	-	0.033	0.032	0.006	0.004
Na	0.079	0.177	0.328	0.087	0.028	0.196	0.178	0.148	0.265
K	1.881	1.798	1.673	1.979	2.039	1.873	1.850	1.522	1.604
Sum	15.666	15.599	15.732	15.931	15.875	15.829	15.790	15.150	15.498
Mg#	0.85	0.84	0.80	0.51	0.42	0.46	0.45	0.59	0.70
Mg/Fe	5.9	5.1	4.1	1.0	0.7	0.9	0.8	1.4	2.3

FeO* = total iron. - = below detection limit estimated as 0.05 wt.%.

Le Bas, 1987) and intrusive carbonatites (Viladkar, 2000). The micas in extrusive carbonatites have low Al_2O_3 (< 13 wt.%) and low TiO_2 (<3 wt.%), similar to fine-grained intrusive carbonatites (alvikite). In contrast, micas in melilitites have high Al_2O_3 (>12 wt. %) and high TiO_2 (> 8 wt.%). Fenites from Loe Shilman have intermediate Al_2O_3 and TiO_2. Most of the Ruri micas fall within the range of micas in extrusive carbonatites from Rangwa and Uyaynah.

Micas in alkaline carbonatite complexes are usually Ba- and F-rich (e g Seifert *et al.*, 2000; Viladkar, 2000; McCormick and Le Bas, 1996). The F content varies sympathetically with MgO, thus decreasing with magma differentiation. Release of F in fenitising fluids is also possible, as testified by the high F in micas from fenites and glimmerites (Seifert *et al.*, 2000).

Amphibole

Brown amphibole with weak pleochroism, several cm long, occurs as large xenocrysts in one carbonatitic tuff (S113). Its composition and

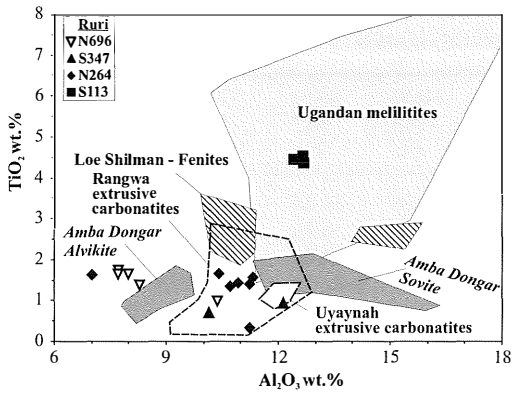

Fig. 7 – Mica Al_2O_3 vs TiO_2 plot. Mica in extrusive carbonatites is Al_2O_3 and TiO_2 poor, those in melilitite Al_2O_3 and TiO_2 rich.

structural formula are close to pargasite (IMA classification, Table 4). It has a high Mg# @ 0.70, and is F-rich. The TiO_2 content reaches 3.8 wt.%, but Cr and Ni are below the detection limits, estimated as 0.05 wt.%. At Deeti, near Kerimasi volcano, Tanzania, the carbonate-rich melilitite tuffs contain large amphibole xenocrysts and amphibole-bearing mantle xenoliths (Johnson *et al.*, 1997). The compositional relationships between pargasite amphibole xenocrysts in melilitite tuff at Deeti and Ruri are compared in terms of Mg# vs TiO_2, with amphibole in Deeti mantle xenoliths and with pargasite xenocrysts occurring in carbonatite lapilli tuffs at Kerimasi (Jones and Church, personal com) (Fig. 8). The Ruri and Deeti pargasite xenocrysts have lower Mg# and higher TiO_2 with respect to amphiboles in the Deeti mantle xenoliths and Kerimasi xenocrysts.

Laser Ablation ICP MS determination of REE in amphibole S113 is reported in Table 4 and plotted on Fig. 9. Overall the amphibole displays enrichment in LREE over MREE and HREE, with a linear enrichment of MREE on HREE and a flat to convex-upward LREE pattern segment. It has a low La/Nd_n ratio (<1) and a high Ce/Lu_n ratio (~ 16-17). Such patterns, have been observed in amphiboles from mantle veins (i.e. Ionov and Hofmann, 1995; Ionov *et al.*, 1997).

TABLE 4

Amphibole composition (sample S113).

analysis	#1	#2
SiO_2	39.88	39.66
Al_2O_3	12.43	12.01
TiO_2	3.78	3.86
FeO*	10.12	10.33
MgO	13.62	13.57
MnO	0.09	0.14
CaO	12.39	12.20
Na_2O	2.42	2.43
K_2O	1.98	2.00
F	0.23	0.23
Total	96.94	96.43
Si	5.989	5.999
$Al^{[IV]}$	2.011	2.001
$Al^{[VI]}$	0.189	0.140
Ti	0.427	0.439
Mg	3.050	3.060
Fe^{2+}	1.271	1.307
Mn	0.012	0.018
Ca	1.994	1.978
Na	0.704	0.712
K	0.379	0.387
Sum	16.026	16.041
Mg#	0.71	0.70
	Aver. of 3	*St dev*
La	12.6	0.26
Ce	32.8	0.44
Pr	5.8	0.12
Nd	29.6	0.62
Sm	6.8	0.62
Eu	1.9	0.06
Gd	5.6	0.36
Tb	0.6	0.04
Dy	3.5	0.19
Ho	0.5	0.06
Er	1.0	0.04
Tm	0.1	0.02
Yb	0.6	0.09
Lu	0.1	0.02
La/Nd_N	0.84	
Ce/Lu_N	16.81	

FeO* = total iron. Analysis by EMPA and LA ICP MS- see text for details.

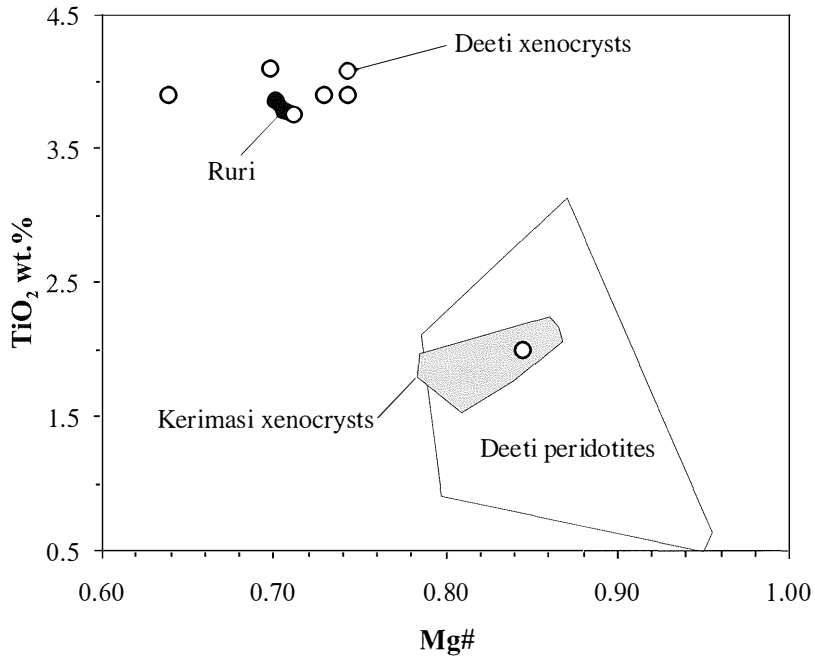

Fig. 8 – Comparison of amphibole at Ruri with amphibole at two extrusive carbonatite localities in Tanzania. Ruri pargasite (S113) is similar to pargasite xenocrysts at Deeti. See text for references.

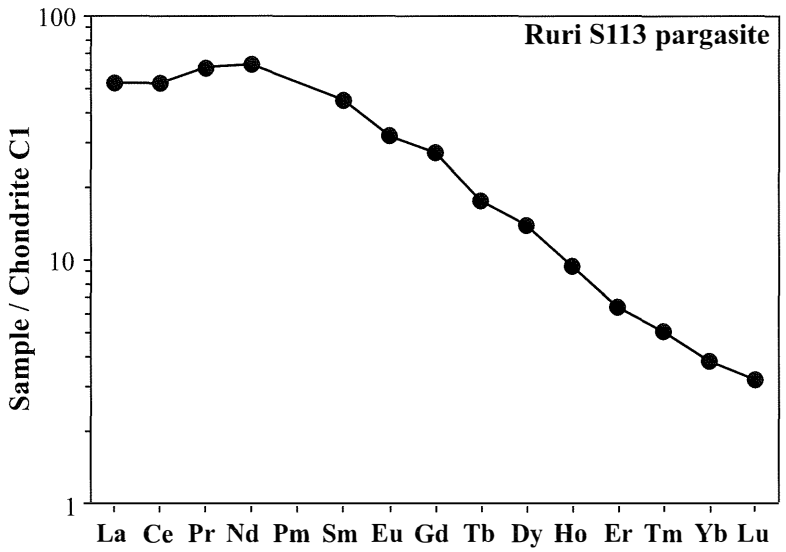

Fig. 9 – REE in Ruri pargasite (S113).

Cr-spinel and Ti-magnetite

Spinel occurs as crystal fragments at the cores of some melilitic lapilli, and as small euhedral crystals scattered in the groundmass of these lapilli (Table 5). Crystals in lapilli cores are Cr-spinel, with Cr_2O_3 up to 37 wt.% (Table 5, anals. 2-5), a composition similar to spinel in mantle xenoliths (Barnes and Roeder, 2001). Interestingly, both Cr-spinel and mantle olivine (see above) have been found in the same sample (S267). In the groundmass the compositions are spinel (Table 5, anal. 6), magnetite with some ulvöspinel solid solution (Table 5, anals. 1, 7-10). The compositions of Ruri magnetite overlap the magnetite compositions in nearby Rangwa extrusive carbonatites and show a similar depletion trend in Al_2O_3 and MgO coupled with increasing Fe (Fig. 10). Such a trend has also been observed in alvikites from Zambia (Bailey and Kearns, 2002). The high Ti content indicates a high temperature of crystallisation.

Melilite and Feldspathoids

As mentioned above, some partially altered melilite crystals preserve the median crack and a peg structure. However, generally, the melilite laths are completely replaced by calcite and/or montmorillonite (XRD identification), and other K-bearing clay minerals (Table 6). Clay minerals also replace pseudomorphs after feldspathoids, possibly nepheline.

Primary carbonate

Carbonate from the Ruri juvenile material is calcite with low MgO, generally <0 3 wt.% (Table 7). It occurs as fiammae, phenocrysts in lapilli and in the fine-grained matrix. The fiammae in sample N264 have high SrO (1.3-1.9 wt. %), BaO (0.6-1.2 wt.%, MnO (1.5-2.4 wt.%) contents, low FeO and negligible MgO (Table 7, anal. 1, Fig. 11). The phenocrysts and the groundmass in the carbonatite lapilli, have high SrO, averaging 1.0 wt.%, but low MnO (Table 7, anals. 2-4). The interlapilli groundmass calcite has variable Sr and Mn (Table 7, anal. 7). Sövite-alvikite fragments have relatively high SrO but low MnO and BaO similar to the lapilli (Tab 7, anal. 5-6). High SrO, BaO and very high MnO and MnO/FeO are considered characteristics of primary magmatic carbonate (Sokolov, 1984).

Secondary carbonate

Low contents of Sr, Ba, and Mn are consistent with a secondary origin for the sparry calcite cement in sample N122 (Table 7, anals. 8-9). In sample S276 the sparry cement is commonly intergrown with fluorite and characterised by very variable SrO and MgO contents, of 0.2 – 1.1 wt.% and 0.3 – 1.4 wt.%, respectively, but low MnO and BaO (Table 7, anal. 9). Sr and Mg may have been mobilised, suggesting a hydrothermal origin. In sample N347, calcite completely replaces melilite in the lapilli and its composition spans that of primary igneous and secondary calcite. Calcite blebs in diopside xenocrysts (N380) have irregular rims of small subhedral magnetite crystals, probably representing a quench mineral and suggesting a magmatic origin for the carbonate. However, this calcite has low SrO (< 0.3 wt.%), low MnO, variable MgO and BaO below detection. This may be the primary composition but, since it is also possible that the carbonate has recrystallised to form a composition consistent with secondary calcite, no firm conclusion can be drawn.

DISCUSSION

Magma fragmentation and pyroclastic structures

At North and South Ruri, most of the extrusive cover has been removed by erosion, leaving conduit-vent breccias and agglomerate, commonly encasing late-emplaced alvikite and sövite. The fragmental nature of the Ruri rocks and the paucity of obvious juvenile components suggest a possible brecciation of the pre-Ruri basement. Further analyses of discrete mineral fragments, lapilli and matrix,

TABLE 5

Representative analyses of spinel group minerals.

sample	S267	S267	S267	S267	S267	S267	S267	S267	N152	N380
mineral	Ti-mag.	Cr-spinel	Spin.	Ti- mag.						
	1	2	3	4	5	6	7	8	9	10
SiO_2	0.10	0.06	0.09	0.11	0.08	0.10	0.09	-	1.34	0.15
Al_2O_3	3.51	44.24	37.16	39.17	24.26	59.46	1.32	1.22	0.67	3.71
TiO_2	13.27	0.11	0.70	0.67	1.08	0.43	10.58	10.84	5.67	13.85
Fe_2O_3	42.37	4.10	9.28	8.46	6.85	7.49	46.02	46.38	52.07	36.86
FeO	30.00	9.71	11.46	11.93	13.49	9.58	38.50	38.79	32.16	34.15
Cr_2O_3	-	20.76	22.30	20.89	37.07	1.56	-	-	-	0.05
MgO	8.02	18.71	17.18	17.18	14.76	20.95	0.82	0.84	0.78	5.14
MnO	0.94	0.14	0.24	0.12	0.09	0.12	0.93	1.00	2.09	0.89
CaO	0.35	-	0.11	0.10	-	-	-	-	1.32	0.24
Total	98.56	97.83	98.52	98.63	97.68	99.69	98.26	99.07	96.10	95.04
Cation calculation based on 32 O										
Si	0.028	0.012	0.020	0.025	0.019	0.020	0.027	-	0.418	0.044
Al	1.176	11.594	10.055	10.506	7.053	14.408	0.475	0.435	0.246	1.312
Ti	2.839	0.018	0.120	0.114	0.199	0.066	2.434	2.474	1.331	3.126
Fe^{3+}	9.074	0.686	1.603	1.449	1.271	1.158	10.595	10.592	12.239	8.326
Fe^{2+}	7.141	1.805	2.200	2.270	2.782	1.647	9.850	9.846	8.400	8.574
Cr	0.006	3.650	4.047	3.759	7.229	0.253	-	-	-	0.011
Mg	3.401	6.202	5.879	5.828	5.426	6.420	0.374	0.379	0.362	2.299
Mn	0.226	0.026	0.046	0.022	0.018	0.020	0.241	0.257	0.552	0.226
Ca	0.106	-	0.026	0.024	-	-	-	-	0.441	0.076
Sum	23.997	23.993	23.996	23.997	23.997	23.992	23.996	23.983	23.989	23.994
Mg#	0.32	0.77	0.73	0.72	0.66	0.80	0.04	0.04	0.04	0.21
Cr#	-	0.24	0.29	0.26	0.51	0.02	-	-	-	0.01
Endmembers										
	S267	S267	S267	S267	S267	S267	S267	S267	N152	N380
	#23	#1	#3	#4	#7	#9	#11	#8	#49	#60
Spi	7.36	72.50	62.90	65.69	44.10	80.37	2.98	2.73	1.54	8.21
Her	-	-	-	-	-	9.73	-	-	-	-
Qa	18.25	0.39	1.76	1.74	2.75	-	0.85	1.05	4.26	10.76
Mfe	-	4.29	7.47	4.01	7.95	-	-	-	-	-
Jac	2.83	-	0.58	0.28	-	0.26	3.01	3.21	6.91	2.83
Usp	17.61	-	-	-	-	1.08	29.92	30.00	17.62	28.90
Mnc	-	0.33	-	-	0.23	-	-	-	-	-
Pic	-	0.05	-	-	10.32	-	-	-	-	-
Chr	0.04	22.45	25.32	23.50	34.65	1.58	0.01	-	0.04	0.07
Mag	53.90	-	1.99	4.77	-	6.99	63.23	63.01	69.62	49.23
Sum	99.95	99.96	99.93	99.96	99.96	99.95	99.97	99.96	99.95	99.96

Fe^{3+}/Fe^{2+} calculated on the basis of charge balance. - = below detection limit estimated as 0.05 wt.%. Endmembers after Stormer (1983): Spi – Spinel $MgAl_2O_4$, Her – Hercynite $FeAl_2O_4$, Qa – Qandilite Mg_2TiO_4, Mfe – Magnesioferrite $MgFe_2O_4$, Jac – Jacobsite $MnFe_2O_4$, Usp – Ulvöspinel Fe_2TiO_4, Mnc – Manganochromite $MnCr_2O_4$, Pic – Picrochromite $MgCr_2O_4$, Chr – Chromite $FeCr_2O_4$, Mag – Magnetite $FeFe_2O_4$.

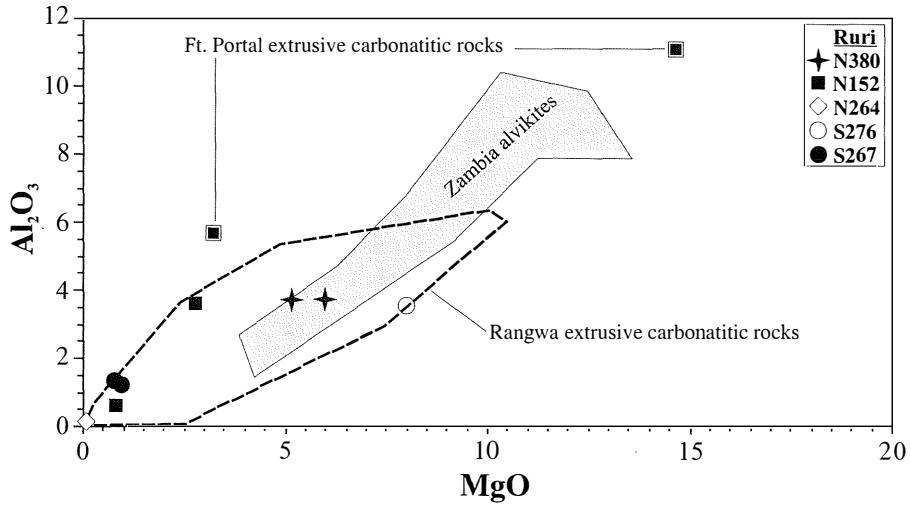

Fig. 10 – Comparison between spinel in Ruri, Rangwa, Fort Portal and Zambia carbonatites.

TABLE 6

Analyses of supposed melilite alteration products.

sample	S236	S276	S276
analysis	1	2	3
SiO_2	57.50	54.80	52.60
Al_2O_3	22.70	17.40	16.40
TiO_2	0.21	0.38	1.16
Fe_2O_3*	2.82	7.54	10.20
MgO	2.34	4.41	6.68
MnO	-	-	0.12
CaO	2.60	3.02	4.68
Na_2O	0.07	-	0.24
K_2O	0.19	0.45	2.20
Total	88.43	88.00	94.28

Fe_2O_3* = total iron. - = below detection limit estimated as 0.05 wt.%.

presented in the previous sections, have enabled us to recognise them as juvenile fragments produced by subvolcanic or deeper magma fragmentation. Only a very few of the brecciated facies may be related to rheomorphism of sub-volcanic dikes (alvikites). All the rest are pyroclastic rocks related to, highly explosive volcanism. Owing to the highly explosive nature of the Ruri volcanic activity, it is presumed that more extrusive material was originally dispersed by the eruptive column and surges over a wider area. The origin and mechanism of such a phenomenon is distinctive and possibly related to the near-primary nature of the magma and rapid emplacement from source to surface.

The Ruri rocks are a mixture of silicate and carbonate juvenile components plus accessory lithics and xenocrysts. The texture of the tuffs is unusual, being modified by this bimodal composition and can be explained by the different viscosities of carbonate and silicate liquids. The latter are clearly co-eruptive at Ruri and thus we have to assume a similar eruption temperature for the two phases, which were physically separated during emplacement. The difference in the texture and structure of the pyroclasts formed by melilitite and carbonatite can easily be explained by the differing viscosities of the separated melts, which causes them to have different rheological behaviour during volcanic processes. Immiscible separation, turbulence, fragmentation and varying shapes and sizes of

TABLE 7

Representative analyses of calcite.

sample	**N264**			**N152**			**S113**	**N122**	**S276**
occurrence	fiammae		trachytoidal lapillus		alvikite		lapillus	sparry calcite	
		pheno	pheno	gr.mass	fragment		gr.mass	cement	
	1	2	3	4	5	6	7	8	9
	1	2	3	4	5	6	7	8	9
SiO_2	0.05	-	-	-	-	-	0.08	-	0.14
FeO*	0.31	-	-	-	-	0.13	0.47	-	-
MgO	0.05	0.34	0.26	0.18	0.12	0.11	0.02	0.17	0.31
MnO	1.57	-	0.11	0.07	-	-	1.74	0.67	-
CaO	55.04	55.2	56.45	55.74	55.77	56.14	54.16	57.94	53.75
SrO	1.88	1.31	0.85	0.91	1.04	0.82	0.18	0.11	0.12
BaO	1.12	0.05	0.22	0.06	0.1	0.06	0.13	-	-
Total	60.02	56.9	57.89	56.96	57.03	57.26	56.78	58.89	54.32

FeO* = total iron. pheno = phenocryst; gr.mass = ground mass. - = below detection limit of about 0.05 wt.%.

volcanic particulates, and the formation of internal structures of the lapilli can be triggered in the magma column by differential viscosity and velocity. Melilitite forms a specific type of lapilli with clear concentric layering. This structure is apparently related to the accretion of glass veneers of melilite-crystallising melt around a solid kernel of olivine or clinopyroxene. This process is related to the higher viscosity and surface tension of melilitite liquid with respect to carbonatite liquid. Melilite would wet easily, in possibly under-cooled conditions, to solid fragments such as mantle debris and xenocrysts. In fact, Ruri melilitite lapilli invariably have a high pressure crystal kernel. It is inferred that magma fragmentation may be early and deep-seated, because CO_2 exsolution can occur at higher pressure than exsolution of supercritical H_2O. In similar material elsewhere, and notably Vulture, Italy, melilitite lapilli have an external rim of carbonatite (Stoppa and Principe, 1998; Stoppa and Woolley, 1996). This can also reflect late separation in subvolcanic conditions (Stoppa *et al.*, this volume). Carbonatite tends to form very small droplets, which were sprayed out during eruption to form the micritic carbonatite matrix of the tuffs. Carbonatite non-nucleated lapilli, which are simply carbonate lapilli, possibly formed by coalescence of smaller drops under volcanic conditions. These lapilli were evidently still plastic during emplacement because they were deformed to fiammae. All the subvolcanic processes must have been high energy, because the rising magma column was able to disaggregate and carry dense mantle debris.

On a global scale, a small proportion of juvenile component compared to the associated brecciated facies and pelletal lapilli seems to be typical of kimberlites and other fluidised breccias that are considered to be a convoy produced by explosive propagation of deep-seated fluids, namely CO_2, towards the surface (Mitchell, 1997). This is supported by the presence of the carbonatite phase with no magma-coolant effects, the ability to carry mantle xenoliths and the absence of any features to suggest blast-triggered surface processes such as phreatomagmatism.

Petrological inferences

Some distinctive features allow us to make some inferences about the melilititic, mantle debris and carbonatitic components in the Ruri pyroclastics. The primary carbonate occurs as extremely fine-grained, turbid material in the matrix, in droplets, lapilli, fiammae and porphyritic lapilli. All of these occurrences are

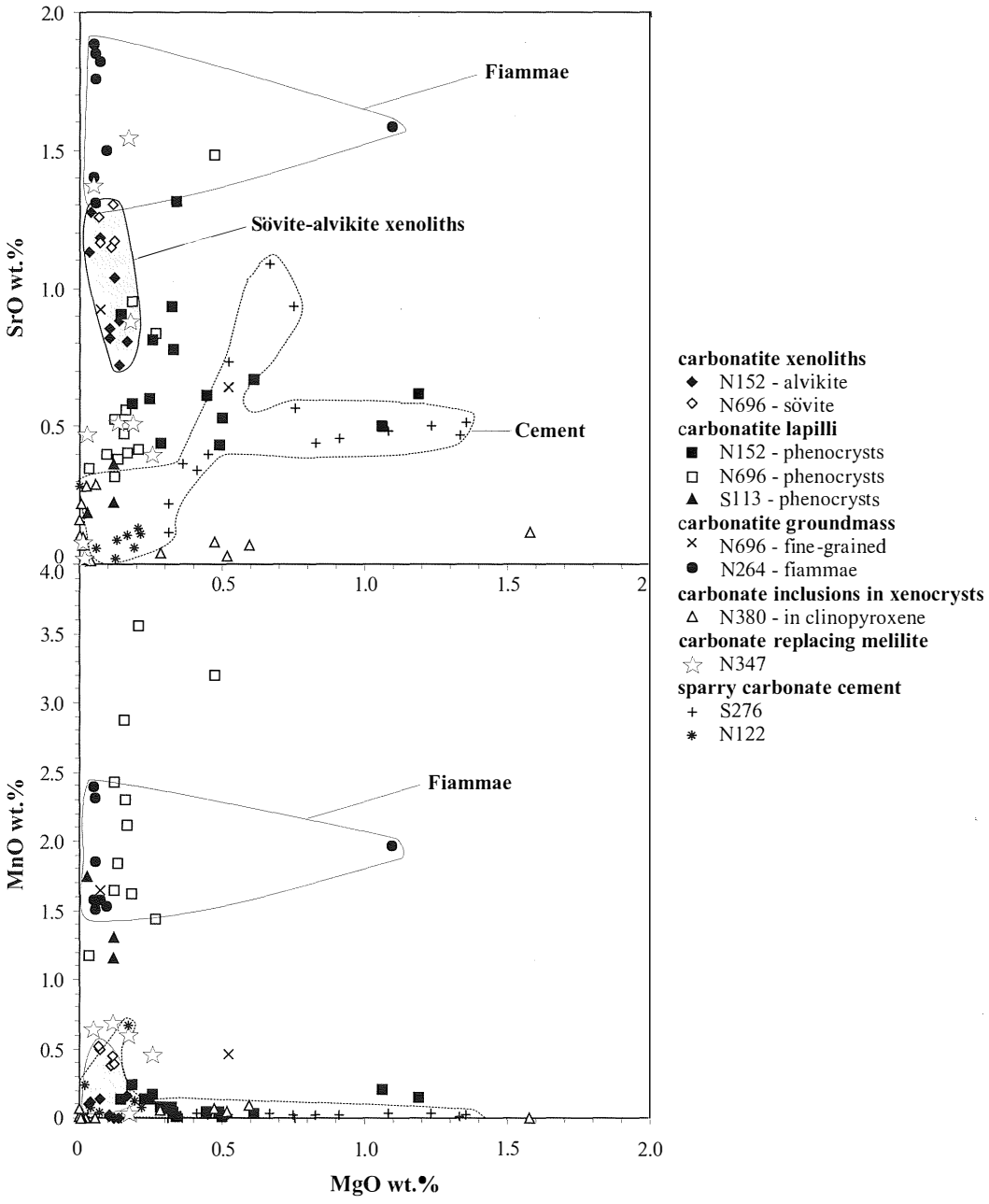

Fig. 11 – Calcite compositions. The calcite forming the fiammae structures (N264) is SrO and MnO rich. Intrusive carbonatite carbonates are similarly SrO rich but MnO poor. There is not a clear discrimination between primary and secondary (cement) carbonate.

melt fragments that formed in a viscous state (acneliths), which indicates the presence of a high temperature quenched or precipitating calcite, liquid phase. However, rapid recrystallisation of igneous carbonates makes the calcite composition typically variable even if higher temperature quenched fragments (fiammae) and most of the calcite laths and fine grained matrix, have high contents of Sr, Ba, Mn expected for primary carbonate in carbonatite.

The liquidus mineral association in the groundmass of the melilititic lapilli is melilite, apatite, magnetite-ulvospinel, mica, salite and possibly some foids. Calcite pseudomorphs after melilite can be distinguished from fresh, monocrystalline laths of calcite by their internal structure and the presence of silicate alteration products. All the rest of the essential minerals seem to be higher pressure xenocrysts or megacrysts; Cr-diopside, olivine, amphibole and Cr-spinel have compositions similar to those found in mantle nodules from other Rift Valley localities.

The eruption of mantle debris, calcite-carbonatite and melilitite is now known to be a common feature of extrusive calcite carbonatites. Several districts have been described where field relationships and geochemistry demonstrate that these three components are a conjugate trio which was co-erupted in a state of physical separation. The best examples are from Katwe-Kikorongo, Uganda (Lloyd *et al.*, 1987), the Italian Ultra Alkaline Province (Stoppa and Woolley, 1996), Eifel, Germany (Lloyd *et al.*, 1991) and Quinling, China (Yu Xuehui *et al.*, 2001). According to the results of experimental petrology calcite carbonatites should not form in the mantle or erupt in isolation. However, there is no doubt about capability of carbonatite to carry mantle fragments. Even diamonds have been recognised in alvikite dikes associated with melilitite-carbonatite tuffisite-diatremes in Uzbekistan (Djuraev and Divaev, 1999). Italian carbonatites, and especially the Polino carbonatite, carry large amounts of ultramafic mantle debris. Owing to their regional association with melilitites, it is supposed that the mantle debris separated from melilitite at the moment of immiscible separation in the upper mantle region and during rapid entrainment in the diatremic conduit to form tuffisites (Stoppa *et al.*, this volume).

There are some clear facts about the natural occurrence of conjugate carbonatite and melilitite. Substantial isotopic and geochemical equilibrium has been demonstrated even though the rocks often have differing mineralogy (Castorina *et al.*, 2000). This fact suggests that the separation is early and then the two liquids follow different crystallisation patterns. Subvolcanic or volcanic processes can re-arrange the two fractions mechanically in either a liquid or a solid state but it seems clear that the two phases tends to remain physically separated.

The relationships between small bimodal carbonatite-melilitite volcanoes and larger alkaline mafic complexes is still unclear. The Ruri centre, close to the large Kisingiri volcano can be compared with other small centres containing high energy facies and more primitive melts and mantle debris nearby to other large alkaline-carbonatite volcanoes. For example, the Deeti tuff cone contains megacrysts of mantle-derived paragasite and clinopyroxene (Johnson *et al.*, 1997) and is just to the northeast of the nephelinite-carbonatite volcano of Kerimasi, within the area of carbonatitic tuffs. The Monticchio Lake diatremes contain mantle xenoliths and consist of melilitite and carbonatite and penetrate the alkaline volcanics at Vulture, Italy (Stoppa and Principe, 1998). There are also some broader examples of a regional association between alkaline rock (leucitites) and melilitite-carbonatite and mantle nodules in the carbonatite melilitite district of Katwe-Kikorongo and leucitite of the Bufumbira district in Uganda (Lloyd *et al.*, 2001) or the carbonatite-melilitite ULUD (Umbria-Latium Ultralkaline District, Stoppa and Woolley, 1996) and leucitite Roman Region in Italy (Cundari, 1994) They could not be strictly cogenetic but a genetic link is likely.

Slight difference in source depth and conditions could explain different occurrences that are produced by completely different mechanisms of magma detachment from the source and propagation through the lithosphere. This is in agreement with the potentially rapid evolution of a melilititic magma to phonolite and carbonatite (Stoppa and Cundari, 1998). It is inferred that diatreme monogenetic volcanoes are linked to the rapid ascent of a single magma batch which has not undergone to any evolution in a crustal magma chamber. Diatremic propagation does not allow magma chamber formation which is, instead, typical of larger stratovolcanoes. Commonly melilititic carbonatitic monogenetic activity is related in time and space at larger volcanoes which have more evolved rocks. Ijolite, syenite, the sövite intrusive suite and phonolite, associated with the Ruri rocks may derive from an olivine melilititic magma similar to that of the adjacent Kisingiri nephelinitic volcano.

CONCLUSIONS

The Ruri heterolithic tuffs are related to opening vent episodes and are mostly formed by country rocks. However, they maintain the physical evidence of a deep seated component such as ultramafic liquid and ultramafic debris. The presence of concentric lapilli with high pressure kernels forming pelletal tuffisites is crucial specific evidence of mantle magma rapidly rising to the surface in a diatremic conduit. It is inferred that the Ruri volcano was produced by the eruption of a melilitite-carbonatite bimodal magma, very rich in juvenile gases, a fact which can explain the high degree of explosivity in this volcano and the absence of lava flows.

The Ruri rocks add another example to the typical calcite carbonatite, melilitite and ultramafic debris association. Unfortunately, Ruri does not offer discrete polycrystalline mantle nodules; they were probably disaggregated during rapid ascent from the mantle source. However, recognition of mantle debris and its association with ijolite-syenite-sövite implies reconsideration of the melilitite-carbonatite role in west Kenya magmatism. The origin of carbonatite-alkaline mafic complexes may rest on a parental carbonatitic-melilititic magma being able to produce eruption of the immiscible pair melilitite and carbonatite or to produce differentiated rocks emplaced at different crustal levels along different polythermal polybaric patterns.

The Ruri melilititic component is not fresh and therefore not suitable for magmatogenetic studies. However, associated mafic minerals permit the hypothesis that the mantle source was similar to that of other melilititic-carbonatitic districts in the Great African Rift.

ACKNOWLEDGMENTS

The visit of Professor Stoppa to The Natural History Museum, London and use of its analytical facilities was funded by the European Commission's Improving Human Potential (IHP) Programme. Terry Williams and John Spratt are thanked for their generous help with EMPA, and Tony Wighton for sample preparation. We are grateful to Prof. Ray Mac Donald and an anonymous referee for the critical comments on the earlier version of the manuscript.

REFERENCES

BAILEY D.K. and KEARNS S. (2002) — *High-Ti magnetite in some fine grained carbonatites and magmatic implications.* Min. Mag. **66**, 379-384.

BARKER D.S. and NIXON P.H. (1989) — *High-Ca, low-alkali carbonatite volcanism at Fort Portal, Uganda.* Contrib. Mineral. Petrol. **103**, 166-177.

BARNES S.J. and ROEDER P.L. (2001) — *The range of spinel compositions in terrestrial mafic and ultramafic rocks.* J. Petrol. **42**, 2279-2302.

CASTORINA F., STOPPA F., CUNDARI A. and BARBIERI M. (2000) — *An enriched mantle source for Italy's melilitite-carbonatite association as inferred by its εNd-Sr isotope signature.* Min. Mag. **64**, 155-169.

CLARKE L.B. and ROBERTS B. (1986) — *Carbonated melilitites and calcitized alkali carbonatites from Homa Mountain western Kenya: a reinterpretation.* Geol. Mag. **123**, 683-692.

CUNDARI A. and FERGUSON A.K. (1982) — *Significance of the pyroxene chemistry from leucite-bearing and related assemblages.* Tsch. Min. Petr. Mitt. **30**, 189-204.

CUNDARI A. (1994) — *Role of subduction in the genesis of potassic basaltic rocks: a discussion paper on the unfashionable side of the role.* Min. Petr. Acta **37**, 81-90

DAWSON J.B., POWELL D.G. and REID A.M. (1970) — *Ultrabasic xenoliths and lava from the Lashaine Volcano, northern Tanzania.* J. Petrol. **11**, 519-548.

DAWSON J.B. and SMITH J.V. (1992) — *Olivine-mica pyroxenite xenoliths from northern Tanzania: metasomatic products of upper mantle peridotite.* J. Volcanol. Geotherm. Res. **50**, 131-142.

DJURAEV A.D. and DIVAEV F.K. (1999) — *Melanocratic carbonatites – New type of diamond-bearing rocks, Uzbekistan.* Mineral deposits: Process to processing. C.J. Stanley et al., (eds), Balkema, Rotterdam 639-642.

KELLER J. (1989) — *Extrusive carbonatites and their significance.* In Bell K (ed): *Carbonatites: genesis and evolution.* Unwin Hyman, London 70-88.

KUSHIRO I. (1960) — *Si-Al relations in clinopyroxenes from igneous rocks.* Am. J. Sci. **258**, 548-554.

IONOV D.A. and HOFMANN A.W. (1995) — *Nb-Ta-rich mantle amphiboles and micas: implications for subduction-related metasomatic trace element fractionations.* Earth Planet. Sci. Lett. **131**, 341-356.

IONOV D.A., GRIFFIN W.L. and O'REILLY S.Y. (1997) — *Volatile-bearing minerals and lithophile trace elements in the upper mantle.* Chem. Geol. **141**, 153-184.

JOHNSON L.H., JONES A.P., CHURCH A.A. and TAYLOR W.R. (1997) — *Ultramafic xenoliths and megacryst from a melilitite tuff cone, Deeti, northern Tanzania.* J. Afric. Earth Sci. **25**, 29-42.

LE BAS M.J. (1962) — *The role of aluminum in igneous clinopyroxenes with relation to their parentage.* Am. J. Sci. 260, 267-288.

LE BAS M.J. (1977) — *Carbonatite-nephelinite volcanism: An African case history.* London, John Wiley & Sons.

LE MAITRE R.E. (2002) — *Igneous Rocks: A Classification and Glossary of Terms*, 2nd edition. Cambridge University Press, Cambridge 236 pp.

LLOYD F.E., NIXON P.H., HORNUNG G. and CONDLIFFE E. (1987) — *Regional K-metasomatism in the mantle beneath the west branch of the East African Rift: alkali clinopyroxenite xenoliths in highly potassic magmas.* In: Nixon PH (ed): *Mantle xenoliths.* John Wiley and Sons, Chichester, pp 641-659.

LLOYD F.E., EDGAR A.D., FORSYTH D.M. and BARNETT R.L. (1991) — *The parageneses of upper mantle xenoliths from the quaternary volcanics south-east of Gees, West Eifel, Germany.* Min. Mag. **55**, 95-112.

LLOYD F.E., WOOLLEY A.R., STOPPA F. and EBY G.N. (2001) — *Phlogopite-biotite parageneses from the K-mafic-carbonatite effusive magmatic association of Katwe-Kikorongo, SW Uganda.* Mineral. Petrol., A.D. Edgar Memorial Volume, 1-24.

LONGERICH H.P., JACKSON S.E. and GUNTER D. (1996) — *Laser ablation inductively coupled plasma-mass spectrometric transient signal data acquisition and analyte contentration calculation.* J. Anal. Atom. Spect. **11**, 899-904.

MCCORMICK G.R. and LE BAS M.J. (1996) — *Phlogopite crystallization in carbonatitic magmas from Uganda.* Canad. Mineral. **34**, 469-478.

MIAN I. and LE BAS M.J. (1987) — *The biotite-phlogopite series in fenites from the Loe Shilman carbonatite complex, NW Pakistan.* Min. Mag. **51**, 397-408

MITCHELL R.H. (1997) — *Kimberlites, orangites, lamproites, melilitites and minettes: a petrographic atlas.* Almaz Press Inc, Ontario, Canada.

NIXON P.H. (1987) — *Kimberlitic xenoliths and their cratonic settings* In: Nixon PH (ed): *Mantle xenoliths.* John Wiley and Sons, Chichester, 215-239.

PASTERIS J.D. (1987) — *Fluid inclusions in mantle xenoliths.* In: Nixon PH (ed): *Mantle xenoliths.* John Wiley and Sons, Chichester, 691-707.

ROSATELLI G. (2002) — *The petrogenesis of carbonatitic rocks and their relation to mantle amphibole and carbonate as exemplified in contrasting volcanoes from Vulture, Italy and Rangwa, Kenya.* PhD Thesis, 239 pp.

ROSATELLI G., WALL F. and LE BAS M.J — *Potassic glass and calcite carbonatite in extrusive carbonatites from the Rangwa caldera of the Kisingiri Volcano* (Submitted).

SEIFERT W., KAMPF H. and WASTERNACK J. (2000) — *Compositional variations in apatite, phloglopite and other accessory minerals of the ultramafic Delitzsch complex, Germany: implication for cooling history of carbonatites.* Lithos **53**, 81-100.

SOKOLOV S.V. (1984) — *Carbonates in ultramafic alkali-rock and carbonatite intrusions.* Geochem. Int. **22**, 150-166.

STOPPA F. and WOOLLEY A.R. (1996) — *The Italian carbonatites: field occurrence, petrology and regional significance* Mineral. Petrol. **59**, 43-67.

STOPPA F. and CUNDARI A. (1998) — *Origin and multiple crystallization of the kamafugite-*

carbonatite association:the San Venanzo-Pian di Celle occurrence (Umbria, Italy). Min. Mag. **62**, 273-289.

STOPPA F. and PRINCIPE C. (1998) — *Eruption style and petrology of a new carbonatitic suite from the Monte Vulture (southern italy): The Monticchio lakes formation.* J. Volcanol. Geotherm. Res. **80**, 137-153.

STORMER J.C. (1983) — *The effects of recalculation on estimates of temperature and oxygen fugacity from analyses of multicomponent iron-titanium oxides.* Am. Mineral. **68**, 586-594.

VILADKAR S.G. (2000) — *Phlogopite as an indicator of magmatic differentiation in the Amba Dongar carbonatite, Gujarat, India.* N. Jb. Miner. Mh. **7**, 302-314.

WOOLLEY A.R., BARR M.W.C., DIN V.K., JONES G.C., WALL F. and WILLIAMS C.T. (1991) — *Extrusive carbonatites from the Uyaynah area, United Arab Emirates.* J. Petrol. **32**, 1143-1167.

WOOLLEY A.R. (2002) — *Igneous silicate rocks associated with carbonatites: their diversity, relative abundances and implications for carbonatite genesis.* Per. Mineral., this volume.

XUEHUI Y., XUANXUE M., ZHONGLI L., ZHAO X., and QI S. (2001) — *Temperature and pressure condition of garnet websterite from west Quiling, China.* Science in China **44**, 150-160.